Proceedings of the IASS Annual Symposium 2017
"Interfaces: architecture . engineering . science"
September 25 - 28th, 2017, Hamburg, Germany
Annette Bögle, Manfred Grohmann (eds.)

Design of ultra-thin composite deployable shell structures through machine learning

Miguel A. BESSA*, Sergio PELLEGRINO+

Graduate Aerospace Laboratories, California Institute of Technology
1200 E California Blvd, Pasadena, CA 91125
*mbessa@caltech.edu
+sergiop@caltech.edu

Abstract

A data-driven computational framework is applied for the design of optimal ultra-thin Triangular Rollable and Collapsible (TRAC) carbon fiber booms. High-fidelity computational analyses of a large number of geometries are used to build a database. This database is then analyzed by machine learning to construct design charts that are shown to effectively guide the design of the ultra-thin deployable structure. The computational strategy discussed herein is general and can be applied to different problems in structural and materials design, with the potential of finding relevant designs within high-dimensional spaces.

Keywords: Buckling, ultra-thin composite shells, machine learning, data mining, data-driven computational framework, design

1. Introduction

The recent resurgence of interest in buckling of slender structures is well documented [1,2]. This trend can be largely explained by the advent of new manufacturing techniques [3] that simplified the fabrication of complex shapes, as well as improved modeling capabilities [4] that leverage the extensive theoretical understanding of buckling [5].

In this article the general data-driven computational framework recently developed in [6] is extended to allow for design and analysis of structures subjected to buckling. This procedure is illustrated by applying it to ultra-thin deployable composite shell structures. The procedure is applicable to other structures (and materials) with different geometries, properties and loading conditions.

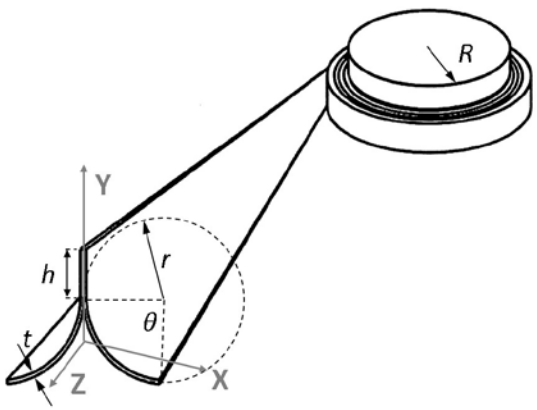

Figure 1: Schematic of TRAC boom architecture (modified from [7]).

Figure 1 shows a schematic of the structure used to illustrate the computational framework henceforth: a triangular rollable and collapsible (TRAC) boom [7] and its packaging behavior. The geometry of this structure is remarkably simple: two tape springs bonded on one end forming a flat region (web) with twice the thickness of the flanges. When packaged, the TRAC boom is flattened (flat cross-section) and rolled around a hub of radius R. The deployed geometry is then fully characterized by the TRAC boom length L and its cross-section parameters: web height h (thickness $2t$), flange radius r, angle θ and thickness t.

The transverse strain caused by flattening the TRAC boom for subsequent rolling it can be predicted as follows [8]:

$$\varepsilon_{flat} = \frac{t}{2r} \tag{1}$$

where typically a strain above 1% would be considered excessive for composite materials. The strain caused by rolling the flattened structure around a hub could also be included, although this strain is usually not the limiting factor since the radius of the hub R used to roll the TRAC booms is large.

The structures were subjected to two separate boundary conditions: bending moment around X leading to compression at the outer edge of the web; and bending moment around Y – see Figure 1. The buckling modes obtained for these two loading conditions occur in distinct regions. When bending around X the web is in compression, while bending around Y causes compression of one flange. Once the buckling load is reached the regions under compression buckle.

The paper is outlined as follows. Section 2 summarizes the data-driven computational framework. Section 3 provides the results obtained from the application of the framework to design TRAC booms with improved buckling behavior. Section 4 presents the conclusions of this work and discusses future directions.

2. Data driven computational framework

The data-driven computational framework developed in [6] conjugates three steps in order to model the relationship between inputs and quantities of interest for materials and structures: 1) Design of Experiments (DoE); 2) computational analyses; and 3) machine learning. The reader is referred to the original publication [6] for a detailed discussion of these steps. The framework is summarized in Figure 2 for structural applications.

The first step (DoE) pertains the sampling of the design/analysis space without a priori knowledge of the relationship between the input variables and the output quantities of interest. The second step concerns the computational analysis of the problem of interest, i.e. predictions of the quantities of interest of the structure for each input point. This leads to the creation of a database with the quantities of interest for each input point, from which the third step – machine learning – can be conducted to learn the relationship between the inputs and outputs. This learning process through artificial intelligence can then be used to create continuous design charts for each quantity of interest.

A particular challenge when using machine learning to establish the relationship between the design inputs and outputs is the need to obtain a sufficiently large database in order to achieve a certain predictive accuracy. The size of the database depends on multiple factors, namely on the choice of methods for each of the three steps of the framework as well as the specific process being analyzed. In mechanics of materials and structures the typical bottleneck is the computational efficiency of the second step – computational analysis of each input point. Here the focus is on nonlinear buckling of deployable structures, where the computational analyses can be completed within reasonable time

(approximately 96 CPU-hours) using the finite element method, without the need for considering reduced order models [9, 10, 11, 12].

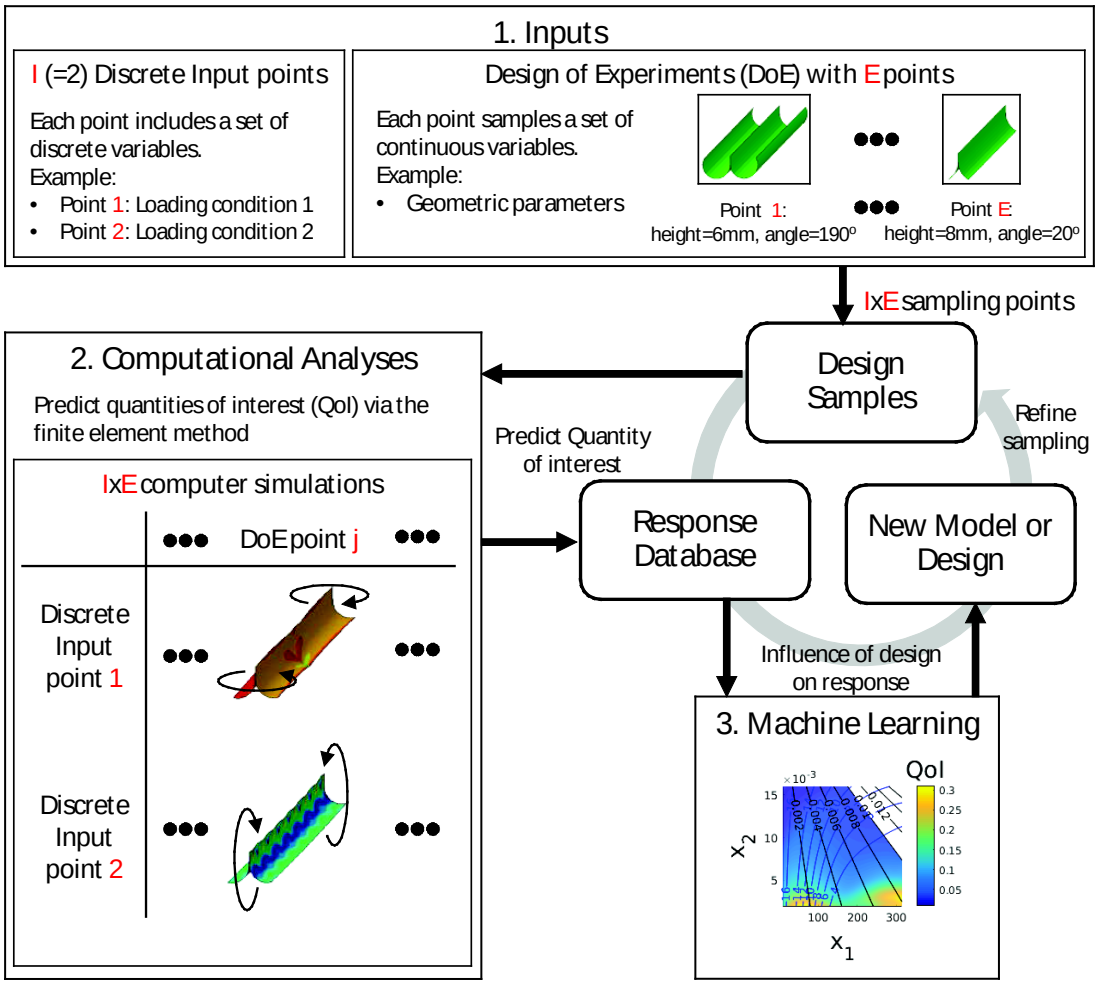

Figure 2: Data-driven framework applied to structural modeling and design (modified from [6]).

3. Design of ultra-thin TRAC booms for improved buckling behavior

The TRAC booms' material is considered to be a composite laminate with stacking sequence $[0^o,90^o]_s$ and nominal post-cure thickness t of *71* µm, where the four composite plies are stacked from a 17GSM unidirectional tape supplied by North Thin Ply Technology (T800 fibers and ThinPreg 120EPHTg-402 epoxy resin). Since the material does not change in this study, the thickness t of the TRAC boom cross-section is kept constant. The total length L is *504* mm of the structure is also constant, as well as the volume V of *1963* mm^3 in order to establish a fair comparison between the different cross-sections. These values coincide with preliminary experiments of a specific geometry of this structure reported in [13], where the nominal cross-section parameters were r*=10.6* mm, θ*=105*°, and h*=8* mm. Note that each geometry in the study described herein is fully characterized by three cross-section parameters r, θ, and h. However, since the volume (mass) of the structures is kept

constant only two of these parameters remain independent (e.g. θ and h) due to the following constraint:

$$r = \frac{V - 2thL}{2\theta tL} \tag{2}$$

With $V \approx 1963$ mm^3, $t=71$ μm, and $L=504$ mm, while the two design descriptors θ (in radians) and h assume different values for different cross-sections. The DoE for this problem follows from defining the bounds for θ and h:

$$h = [2,16]mm \quad , \quad \theta = [10^o, 315^o] \tag{3}$$

As proposed in [6] the DoE can be efficiently performed by a Sobol sequence [14] for general n-dimensional spaces. This method produces a nonuniform space-filling design where different hyperplane projections do not lead to coincident points – properties that have been shown to facilitate the machine learning process [6]. Figure 3 presents the 1,000 DoE points obtained from a random Sobol sequence of the two design parameters used in the investigation of the influence of the structure cross-section on its initial buckling behavior. The solid red circles correspond to the first 20 points of the Sobol sequence used, demonstrating that this is a nonuniform space-filling design that leads to successive refinements of the space with increasing number of points.

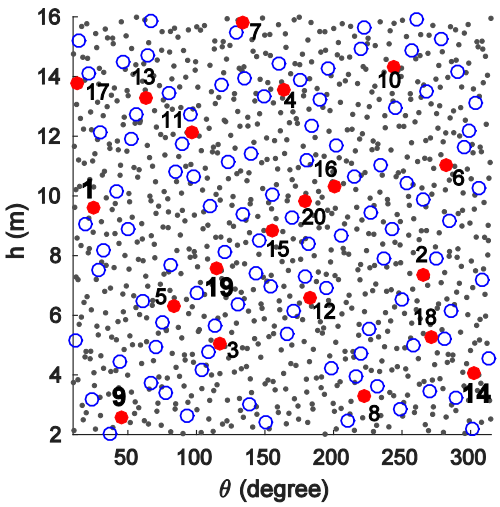

Figure 3: Design of Experiments to determine the influence of the TRAC boom geometries on the initial buckling behavior of the ultra-thin composite structure. The solid red circles correspond to the first 20 points of the Sobol sequence and are labeled with the corresponding sequence number. The black dots correspond to the remaining 880 points, and the last 100 points are shown as blue circumferential markers.

The subsequent step in the data-driven framework after defining the DoE is the computational analysis of each DoE point. The structures were subjected to two separate boundary conditions: bending moment around X leading to compression at the outer edge of the web; and bending moment around Y – see Figure 1. These boundary conditions correspond to the two "Discrete Input points" in Box 2 of Figure 2, such that the response of all the different geometries defined by the DoE points shown in Figure 3 are analyzed for each boundary condition (2 in this case). Geometric variations of the structure are expected to lead to competing effects for these two boundary conditions. For example, adding/removing material in the web has significant impact on the bending stiffness and buckling of the structure for bending around X, but less impact for bending around Y because the web is in the neutral plane in this case. Note, however, that this influence is less intuitive when considering that the

structures have constant volume, because the material that is added in the web needs to be respectively removed in the flanges, which alters the bending stiffness and local curvature of the structure. The actual influence of r, θ, and h is not trivial to predict analytically due to the fact that the structures are ultra-thin, leading to localized buckling modes instead of global modes.

The following procedure is automated for predicting the first bifurcation point of structures undergoing nonlinear buckling:

1. Linear bifurcation analysis of the undeformed configuration of the structure. This provides an initial prediction for the first bifurcation point and buckling modes;
2. Static analysis under displacement control without stabilization until the simulation stops or the previously determined bifurcation point is reached;
3. Sequential linear bifurcation analyses starting from the last available increment of the static analysis until reaching an increment where the bifurcation point can be predicted, i.e. an increment where the structure is not on the postbuckling regime but where it is close to the bifurcation point.

The outlined procedure was implemented such that it could be performed automatically and in parallel for different input DoE points. The output quantities of interest obtained from the simulations, e.g. moments and angles at the two ends, are stored in a database that is then used for the machine learning process.

The machine learning process for this study is simplified because there are only two input variables per boundary condition, and the quantities of interest have negligible noise (no geometric imperfections). In this case a small database is appropriate, favoring the use of the Gaussian process method [15] as opposed to methods such as artificial neural networks [16]. This was shown in [6] with a comparison of the data-driven framework for higher dimensional design spaces using both Gaussian process (also known as kriging) and neural networks. The reader is referred to the work of Rasmussen and Williams [15] for detailed discussions on the Gaussian process, and to Demuth et al. [16] on artificial neural networks.

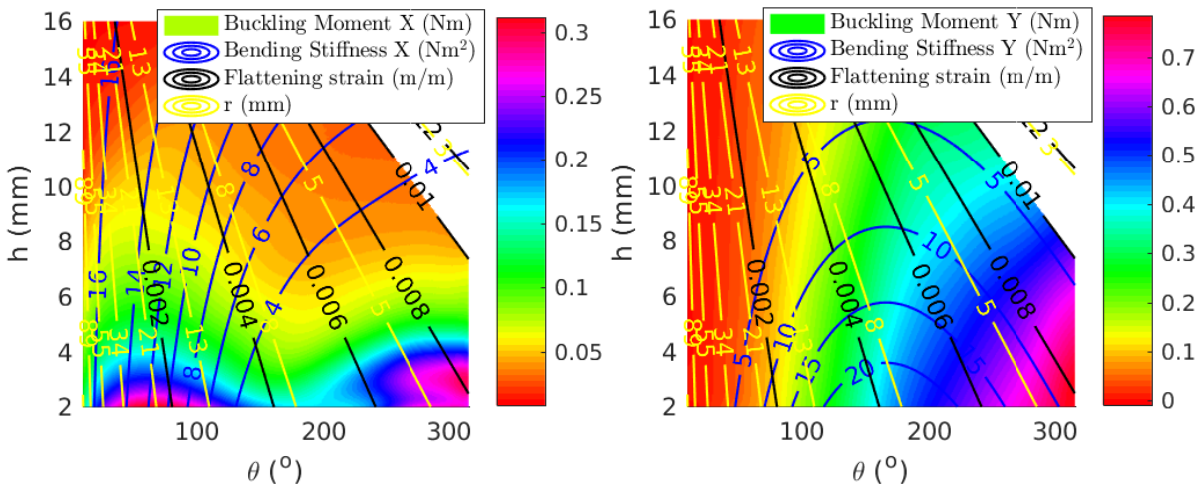

Figure 4: Design charts obtained for the variation of the initial buckling moments in X (left) and Y (right) as a function of two cross-section parameters (θ and h).

Construction of design charts for the quantities of interest follows from the machine learning process. Figure 4 shows the buckling moment obtained at the first bifurcation point of the idealized structures

for the different cross-sections. The figure also includes contour lines of the transverse strain ε_{flat} caused by flattening the structure for packaging given by equation (1), the bending stiffness calculated from the moment-angle response, and the radius of the flanges calculated from equation (2).

Observing Figure 4 one can identify that the maximum buckling moment does not occur for regions with maximum bending stiffness for both boundary conditions. This behavior occurs due to the presence of local buckling modes, justifying the use of computational analyses to find better designs instead of analytical predictions. From the figure it is also clear that constraining the flattening strain below 1% does not significantly limit the design space, which is also a direct consequence of the thin nature of the structure. Interestingly, there is a common region of the design space that maximizes the initial buckling moment for both loading conditions. This region occurs at large flange angles and small web heights, at the expense of those structures having low bending stiffness around X.

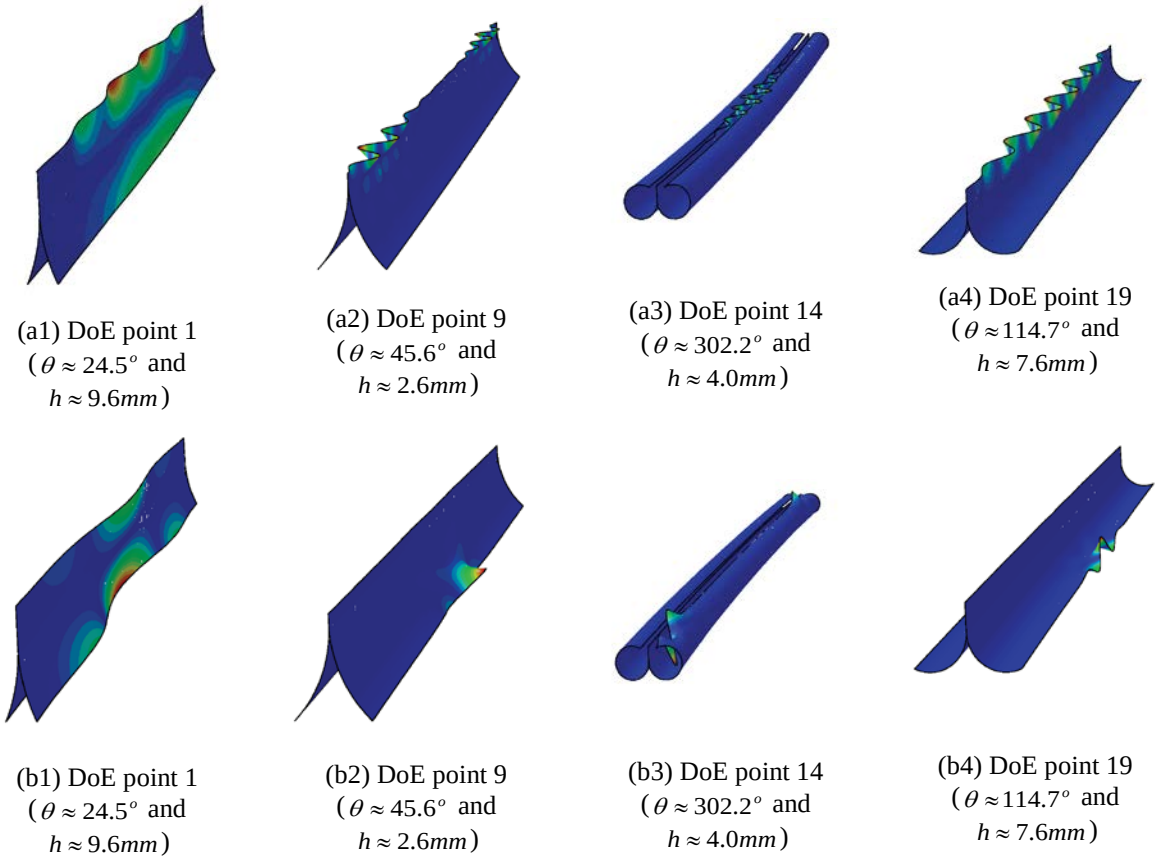

Figure 5: Buckling modes observed for different geometries subjected to two loading conditions: bending around X causing compression of the web (top row labeled a); and bending around Y with buckling of one flange (bottom row labeled b). From left to right the geometries shown correspond to DoE points 1, 9, 14 and 19 shown in Figure 3. The modes are scaled such that the maximum displacement component is 5 mm for all cases.

Figure 5 shows the buckling modes corresponding to 4 DoE points shown in Figure 3. Focusing first on the modes obtained by bending the structures around the X axis (top row labeled with a), one can see that DoE point 9 (a2), and DoE point 14 (a3) show localized buckling modes, as opposed to the more global modes seen around the top of the web for the other geometries. The buckling behavior is improved in point 9 by localizing the deformation at the ends of the structure, while for point 14 it is improved by localizing it in the center after a more compliant behavior in this bending condition. Focusing now on the modes obtained by bending the structures around the Y axis (bottom row labeled

b), one can see that only point 14 (b3) shows the localization of deformation at the ends of the structure, justifying the fact that only this geometry is in the region of the design chart with a higher buckling moment in Y.

Therefore, DoE point 14 corresponds to the best design of the 4 geometries shown in Figure 5, and is within the optimal region found in the design charts. In general, one can conclude that designs with large flange angles and small web heights are the most effective when aiming to increase both buckling loads for constant mass of the structure. If the design goal is different, then the design charts can be used to optimize the structure for other applications, e.g. maximum bending stiffness achieved for a desired minimum buckling strength.

4. Conclusion

A general data-driven computational framework was extended to analyze the buckling behavior of ultra-thin composite TRAC booms with different cross-sections and constant mass. The buckling modes of these deployable shell structures were shown to vary significantly with the geometry of the booms. These differences cause variations on the buckling response that do not scale linearly with the bending stiffness of the structures. Such counter-intuitive variations can be well captured by machine learning, from which design charts can be trivially obtained.

Performance improvements were achieved by finding geometries with localized buckling towards the ends of the booms. The design charts show that maximizing both buckling moments of the structure is possible by considering cross-sections with large flange angles and short web heights, as seen in Figures 5 (a3) and (b3). This conclusion, however, is valid under an important simplifying assumption: the structures were assumed to be perfect, i.e. without imperfections. Future work on the imperfection-sensitivity of these structures for both buckling and postbuckling behavior will be crucial to assess how these findings can be useful in practice.

Acknowledgements

The authors acknowledge financial support from the Northrop Grumman Corporation. Comments of an anonymous reviewer are gratefully acknowledged.

References

[1] N. Hu, R. Burgueño, Buckling-induced smart applications: recent advances and trends, Smart Materials and Structures 24 (6) (2015) 063001.

[2] P. M. Reis, A perspective on the revival of structural (in)stability with novel opportunities for function: From buckliphobia to buckliphilia, Journal of Applied Mechanics 82 (11) (2015) 111001–111001–4.

[3] S. Kalpakjian, S. R. Schmid, K. V. Sekar, Manufacturing engineering and technology, Pearson Upper Saddle River, NJ, USA, 2014.

[4] X. Bai, M. A. Bessa, A. R. Melro, P. P. Camanho, L. Guo, W. K. Liu, High-fidelity micro-scale modeling of the thermo-visco-plastic behavior of carbon fiber polymer matrix composites, Composite Structures 134 (2015) 132 – 141.

[5] Z. P. Bažant, L. Cedolin, Stability of structures: elastic, inelastic, fracture and damage theories, World Scientific, 2010.

[6] M. Bessa, R. Bostanabad, Z. Liu, A. Hu, D. W. Apley, C. Brinson, W. Chen, W. Liu, A framework for data-driven analysis of materials under uncertainty: Countering the curse of

dimensionality, Computer Methods in Applied Mechanics and Engineering 320 (2017) 633 – 667.

[7] T. W. Murphey, J. Banik, Triangular rollable and collapsible boom, US Patent 7,895,795 (Mar. 1 2011).

[8] T. W. Murphey, D. Turse, L. Adams, TRAC boom structural mechanics, in: AIAA SciTech Forum, American Institute of Aeronautics and Astronautics, 2017, pp. –.

[9] J. Michel, P. Suquet, Nonuniform transformation field analysis, International Journal of Solids and Structures 40 (25) (2003) 6937 – 6955, special issue in Honor of George J. Dvorak.

[10] G. Berkooz, P. Holmes, J. L. Lumley, The proper orthogonal decomposition in the analysis of turbulent flows, Annual review of fluid mechanics 25 (1) (1993) 539–575.

[11] F. Chinesta, A. Ammar, A. Leygue, R. Keunings, An overview of the proper generalized decomposition with applications in computational rheology, Journal of Non-Newtonian Fluid Mechanics 166 (11) (2011) 578 – 592.

[12] Z. Liu, M. Bessa, W. K. Liu, Self-consistent clustering analysis: An efficient multi-scale scheme for inelastic heterogeneous materials, Computer Methods in Applied Mechanics and Engineering 306 (2016) 319 – 341.

[13] C. Leclerc, L. L. Wilson, M. A. Bessa, S. Pellegrino, Characterization of ultra-thin composite triangular rollable and collapsible booms, in: AIAA SciTech Forum, American Institute of Aeronautics and Astronautics, 2017, pp. –.

[14] I. M. Sobol, Uniformly distributed sequences with an additional uniform property, USSR Computational Mathematics and Mathematical Physics 16 (5) (1976) 236–242.

[15] C. E. Rasmussen, C. K. I. Williams, Gaussian Processes for Machine Learning (Adaptive Computation and Machine Learning), The MIT Press, 2005.

[16] H. B. Demuth, M. H. Beale, O. De Jess, M. T. Hagan, Neural Network Design, 2nd Edition, Martin Hagan, USA, 2014.